Microwave Absorption Characteristics of Composites with Tungsten Coated Filler Particles

Thomas C. Maloney
Center for Nondestructive Evaluation
Iowa State University
Ames, IA 50011-3042, USA

Nicola Bowler and **Nathan L. Fischer**
Department of Materials Science and Engineering
Iowa State University
Ames, IA 50011-2300, USA

ABSTRACT

This study compares the dielectric relaxation, measured at microwave frequencies, of composites made with four distinct types of filler particles. The particles studied are 3M™ glass bubbles, with diameter approximately 60 μm, sputter coated with tungsten. Prior to sputter coating, one batch of glass bubbles was dried at 150 °C and another at 350 °C. The drying process removes bound water from the de-aggregating agent (Volan®) used to coat the glass bubbles. Of these two batches, some particles were further coated with aluminum oxide (AlOx) to prevent conduction between the particles when in contact. To measure the permittivity, the particles were dispersed in a matrix of paraffin wax at various volume fractions. The electromagnetic properties were measured in the frequency range 2 to 18 GHz using a 7 mm coaxial reflection/transmission line method. Dielectric loss was observed in this frequency range for all four types of filler particle. The composites containing the particles coated with AlOx were observed to have a higher real and imaginary relative permittivity than those containing non-AlOx-coated particles. For AlOx-coated particles, the drying temperature of 150 °C yielded stronger relaxation than that of 350 °C. This behavior is attributed to traces of bound water remaining in the particles dried at 150 °C and its effect on the morphology of the tungsten layer in these particles.

Index Terms — Composite material, dielectric permittivity, microwaves, multi-layered filler particles.

1 INTRODUCTION

IN the past few decades, electromagnetic microwaves have played an increasing role in man's technological achievements and composite materials capable of absorbing microwave radiation are becoming an increasingly important resource. These composites find application in shielding of electronic components, reduction of cross-talk in cell phones, radar absorption and to control heat distribution in microwave-assisted curing or in domestic cooking.

Composite materials dedicated to microwave absorption are often composed of iron filler particles dispersed in a matrix [1]. The non-magnetic, metal-coated particles studied in this article are significantly less dense than iron particles (0.2 rather than 7.8 g/cm^3), which can be an advantage in some applications. They also allow greater control of the extent of electromagnetic absorption and the frequency at which it occurs, by adjustment of metal coating thickness, conductivity, and particle volume fraction. The design of microwave-absorbing composite materials utilizing coated filler particles is discussed in [2].

Figure 1 shows the theoretical performance of composites with three types of spherical filler particles; solid tungsten, tungsten-coated glass microbubbles and similar metal-coated microbubbles with reduced conductivity, as may be the case in a thin metal film [3]. Assuming that the particles are significantly smaller than the wavelength of the incident electromagnetic field, the relative permittivity of the composite, ε, can be calculated from the following effective medium formula [4].

$$\frac{\varepsilon - \varepsilon_m}{\varepsilon + 2\varepsilon_m} = f \frac{(\varepsilon_1 - \varepsilon_m) + (2\varepsilon_1 + \varepsilon_m)g_2(\varepsilon_k, a_k)}{(\varepsilon_1 + 2\varepsilon_m) + 2(\varepsilon_1 - \varepsilon_m)g_2(\varepsilon_k, a_k)} \quad (1)$$

$k = 1, 2$ and

$$g_2 = \frac{\varepsilon_2 - \varepsilon_1}{\varepsilon_2 + 2\varepsilon_1} \left(\frac{a_2}{a_1} \right)^3 \qquad (2)$$

In equations (1) and (2), the filler particles are assumed to consist of a spherical core (region 2, radius a_2) coated with a uniformly thick surface layer (region 1, radius a_1) as shown in Figure 2. These regions have relative permittivity ε_2 and ε_1, respectively, and the matrix material has relative permittivity ε_m. If the permittivity of any of the constituents is complex, then ε will also be complex. For time-harmonic electric field excitation that varies as the real part of $\exp(j\omega t)$,

$$\varepsilon = \varepsilon' - j\varepsilon'', \quad j = \sqrt{-1} \qquad (3)$$

and, for a metal with conductivity σ, the relative permittivity is given by $\varepsilon = 1 - j\sigma/(\omega\varepsilon_0)$ where $\varepsilon_0 = 8.85 \times 10^{-12}$ F/m is the permittivity of free space.

Practically speaking, the ability of a material to absorb electromagnetic radiation depends on many factors, including the geometry of the part and the reflectivity at its surface. Assuming that microwaves do penetrate the material surface, however, energy is absorbed and dissipated as heat when the polarization of the material is out of phase with the applied electric field. For this reason, the phase angle δ defined $\tan \delta = \varepsilon''/\varepsilon'$ is known as the loss tangent of the material. A maximum in ε'' indicates a maximum in the absorbing ability of the material. The calculated values shown in Figure 1 predict that the dielectric loss of the composite formed with solid tungsten particles occurs at a higher frequency than that of glass microbubbles coated with tungsten of the same conductivity. Decreasing the conductivity of the tungsten coating further decreases the frequency ν_{max} at which the maximum dielectric loss occurs.

This paper assesses the suitability of tungsten-coated glass microbubbles as filler particles in composites for microwave absorption. The real and imaginary relative permittivity of various composites is measured in the frequency range 2 to 18 GHz by a transmission-line method and the resulting dielectric relaxation is analyzed.

2 MATERIALS AND METHOD

2.1 FILLER PARTICLES

Relevant physical properties of the filler particles are listed in Table 1. The particles studied are 3M™ Glass Bubbles A20/1000, with mean radius approximately 30 μm, sputter coated with tungsten to a nominal coating thickness of 3 nm [8]. The A20 glass bubbles have a thin surface layer of Volan® bonding agent [8], an organo-metallic film, to prevent aggregation of the powder.

Prior to sputter coating, the A20 glass bubbles were heated for approximately 24 h to drive off moisture. One set of samples was dried at 150 °C and the other at 350 °C.

The particles were then transferred immediately to the sputtering chamber. At the higher temperature the organo-metallic film on the A20 bubbles was observed to change color from green to brown [8]. The film consists of Werner-type chromium complexes of methacrylic acid in isopropanol that bond strongly to glass surfaces and aid in the application of thermosetting resins [9, 10]. The visible change in the Volan® coating suggests subsequent differences in the way that the tungsten film deposits on the particles during the sputter-coating process, and consequently a different structure and film conductivity. A scanning electron microscope (SEM) image of one set of particles is shown in Figure 3.
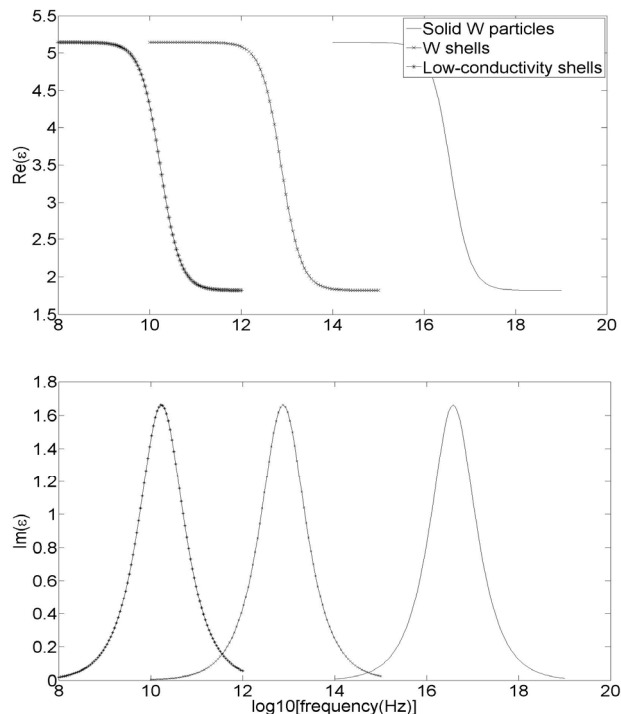

Figure 1. Computed ε' and ε'' for three different filler types: i) spherical solid tungsten particles ($\sigma = 17.7$ MS/m), ii) 3M™ Glass Bubbles A20 with a tungsten coating and iii) as for ii) but with reduced shell conductivity ($\sigma = 40$ kS/m). The calculations were made using an effective medium theory for multilayered filler particles, equation (1), assuming that the filler particles have uniform size with core radius $a_2 = 30$ μm and coating thickness $a_1 - a_2 = 3$ nm. Filler volume fraction $f = 0.3$. The matrix is paraffin wax with $\varepsilon_{wax} = 2.25 - j\, 0.000563$.
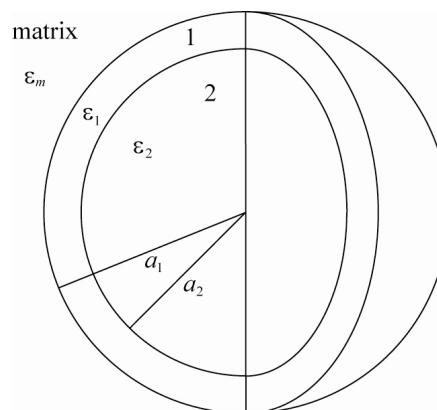

Figure 2. Schematic diagram of a coated, spherical particle.

Table 1. Properties of the A20 Glass Microbubbles, Tungsten Layer and Aluminum Oxide Coating.

| Parameter	Value	Source
Coated Particle		
Density (g/cm^3)	0.20 ± 0.06	calculated from densities and thickness of core particle, W and AlOx
Crush pressure (MPa)	6.89	Assumed to be same as core particle [5]
Core Particle	Glass Microbubble	3M™ Scotchlite™ A20
Density (g/cm^3)	0.2	[5]
10th percentile radius (μm)	15	[5]
50th percentile radius (μm)	30	[5]
90th percentile radius (μm)	50	[5]
Shell material	Soda-lime-borosilicate glass	[5]
Shell density (g/cm^3)	2.5	[6] estimated from values for A and E glass
Shell thickness (μm)	1.65	Calculated from particle and shell densities for mean particle size
Permittivity (100 MHz)	1.4 ± 0.1	[5]
Shell real permittivity	4.8	[7], Pyrex, 25°C, 10GHz
Shell loss tangent (x10^4)	98	[7], Pyrex, 25°C, 10GHz
Core material	Air	Assumed
Tungsten Coating		
Thickness (nm)	3	[8]
Bulk conductivity (MS/m)	17.7	[9]
Density (g/cm^3)	19.3	[9]
Alumina Outer Coating		
Thickness (nm)	3	[8]
Real permittivity	8.79	[7], Coors, 25°C, 10GHz
Loss tangent (x10^4)	18	[7], Coors, 25°C, 10GHz
Density (g/cm^3)	3.97	[9]

The depth resolution of SEM (approximately 4.5 nm) was not sufficient to permit direct observation of possible differences in the nature of the tungsten coating which is nominally 3 nm thick.

Two sets of samples were further coated with aluminum oxide, which serves as a barrier to electrical conduction between adjacent particles. Hence, four different particle types are studied here, as listed in Table 2. The two samples not coated with aluminum oxide were stored under argon prior to use, to inhibit oxidation of the tungsten coating.

Table 2. Tungsten-Coated Particle Types.

Filler	Drying Temperature of A20 Microbubbles (°C)	AlOx Coating Thickness (nm)
AlOx-W-A20-150	150	≈ 3
AlOx-W-A20-350	350	≈ 3
W-A20-150	150	0
W-A20-350	350	0
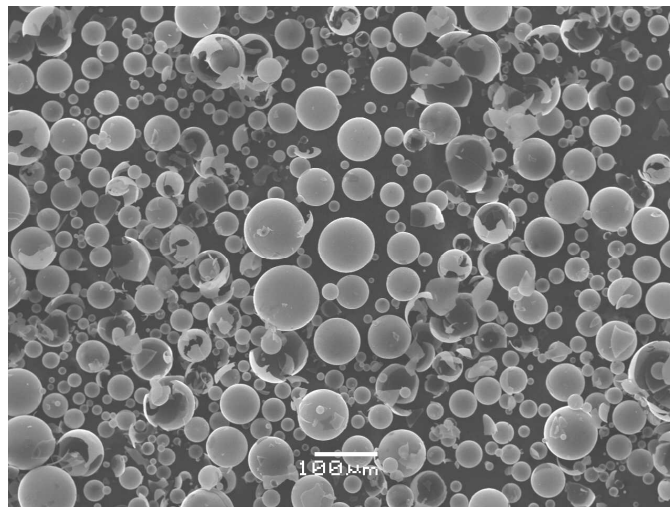
Figure 3. SEM image of AlOx-W-A20-350 particles taken with 20 keV electron beam energy.

2.2 SAMPLE FABRICATION

The filler particles were mixed with paraffin wax at various volume fractions, from 0 to 0.6 volume fraction of filler, to create master batches. The wax and particle mixture was heated at a temperature slightly higher than that of the melting point of the wax (65 °C). The batches were then removed from the heat and manually stirred as they cooled in order to disperse the particles as evenly as possible in the wax. From the master batches, an appropriate amount of material was weighed for fabrication of individual 7 mm coaxial transmission-line samples. Three samples were made for each volume fraction, f. The dominant source of uncertainty in f, estimated to be less than 0.01 based on mass measurements before and after sample fabrication, is the uncertainty in the density of the coated particle, Table 1. Sufficient material for each individual sample was placed into a mold heated to 50 °C and pressed under 11.8 kg of weight for approximately 5 minutes. In this way, air bubbles were removed from the sample without exceeding the crush pressure of the particles, see Table 1. Special care was taken, when fabricating the samples with W-A20 filler particles, to incorporate the particles into the matrix within minutes of exposure to air in order to minimize the likelihood of oxidation of the outer tungsten coating. The nominal length of the samples, L, ranged between 1 and 3 mm. The actual sample length was measured using a digital micrometer with instrument uncertainty ± 0.9 μm. The length was measured at three points on the sample and the readings averaged to reduce error due to variation in L across each sample.

2.3 PERMITTIVITY MEASUREMENT

The permittivity of the samples in the frequency range 2 to 18 GHz was measured using a reflection/transmission line method [12], employing a 7 mm-coaxial-airline sample holder. An Anritsu vector network analyzer, model 37347C, was used to record the S-parameters of reflection and transmission as described by Baker-Jarvis [12].

The measured S-parameter data was analyzed using a root-finding scheme based on the following equation [12].

$$\frac{S_{11}S_{22}}{S_{12}S_{21}} = \frac{\left(1-\dfrac{\varepsilon}{\mu}\right)^2}{\dfrac{4\varepsilon}{\mu}}\sinh^2(\gamma L) \tag{4}$$

In equation (4), the S_{ij} are measured S-parameters, ε and μ are the *relative* permittivity and permeability of the material respectively and

$$\gamma = j\sqrt{\frac{\omega^2\mu\varepsilon}{c_0^2}} \tag{5}$$

where $\omega = 2\pi v$ is the angular frequency of the applied electromagnetic wave and c_0 is the speed of light in free space. This algorithm works well for non-magnetic materials where $\mu = 1$ and ε is the only unknown in equation (4). It also allows

for the position of the sample in the holder to be disregarded. This greatly simplifies the measurement process since the experimental uncertainty associated with sample positioning is eliminated. The well-known Nicholson-Ross-Weir (NRW) algorithm could also be used to analyze the S-parameter data. This algorithm yields both permeability and permittivity data, with the cost of having to know the sample position in the holder. The NRW method also suffers from instability when the length of the sample is a half multiple of the electromagnetic wavelength, λ, in the sample material [12].

3   RESULTS AND DISCUSSION

3.1 MEASURED PERMITTIVITY

Figures 4 to 7 show the measured real and imaginary relative permittivity versus frequency for the four filler particle types studied here; AlOx-W-A20-150, AlOx-W-A20-350, W-A20-150 and W-A20-350 respectively, for volume fractions in the range 0 to 0.6. While measurements were made on three sets of samples for each filler type, a single representative data set for each is shown in these figures. It is evident that a broad dielectric relaxation is partially visible in this frequency range for composites with all four filler particle types. As the volume fraction of the filler particles increases, the permittivity and strength of the dielectric relaxation also increase, in qualitative agreement with theoretical predictions for such systems [13,14]. At 10 GHz, $\varepsilon_{wax} = 2.25 - j\,0.000563$ [7]. It is clear from Figures 4 to 7 that the known value of the real part of ε_{wax} is reproduced very well by the data. The imaginary part of ε_{wax} is below the resolution of this broadband measurement method (± 0.05) [13], which means that some measured values of ε''_{wax} appear negative (e.g. Figures 6 and 9) although in fact $\varepsilon''_{wax} = 0.000563$.

Results for all four particle types are plotted together in Figure 8 for $f = 0.6$. In Table 3, the frequency v_{max} at which the maximum dielectric loss occurs, the peak value ε''_{max}, and the value of ε' at the lowest frequency measured here (2 GHz) are tabulated for the curves shown in Figure 8, for ease of comparison. Uncertainties quoted in Table 3 are standard deviations calculated from measurements made on three nominally identical samples.

3.2 ALUMINUM OXIDE COATING

Comparing measured permittivity values for the composites made with the AlOx-W-A20 particles (Figures 4 and 5) with those made with W-A20 particles (Figures 6 and 7), it is observed that both ε' and ε'' are significantly greater with the presence of the AlOx coating, than without. This is because the dielectric relaxation is due to interfacial polarization and, in the cases where no insulating barrier exists between closely-packed particles, charge can leak from particle to particle, weakening the inter-particle capac-
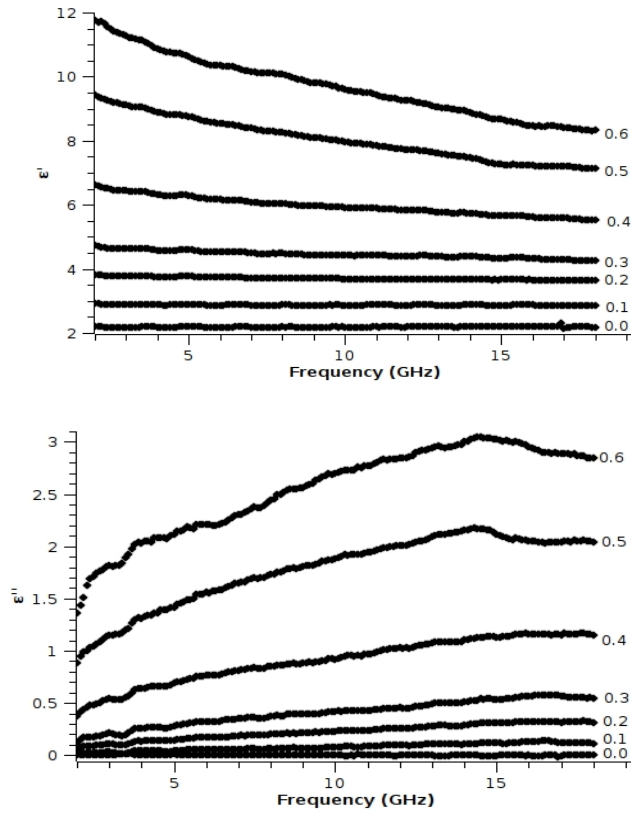
Figure 4. Measured ε' and ε'' versus frequency for composites with AlOx-W-A20-150 filler particles in paraffin wax, for various values of filler volume fraction f.

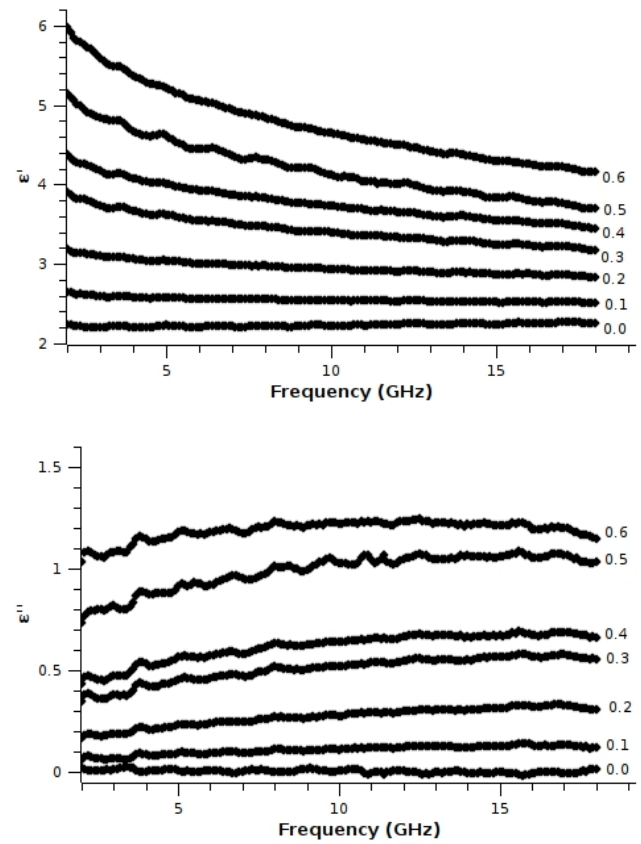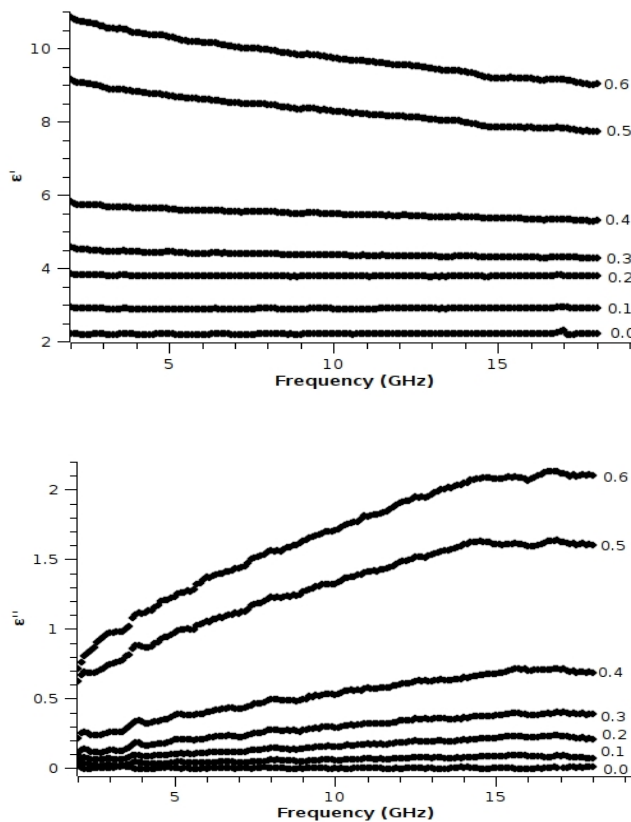**Figure 6.** As for Figure 4 but with W-A20-150 filler particles.

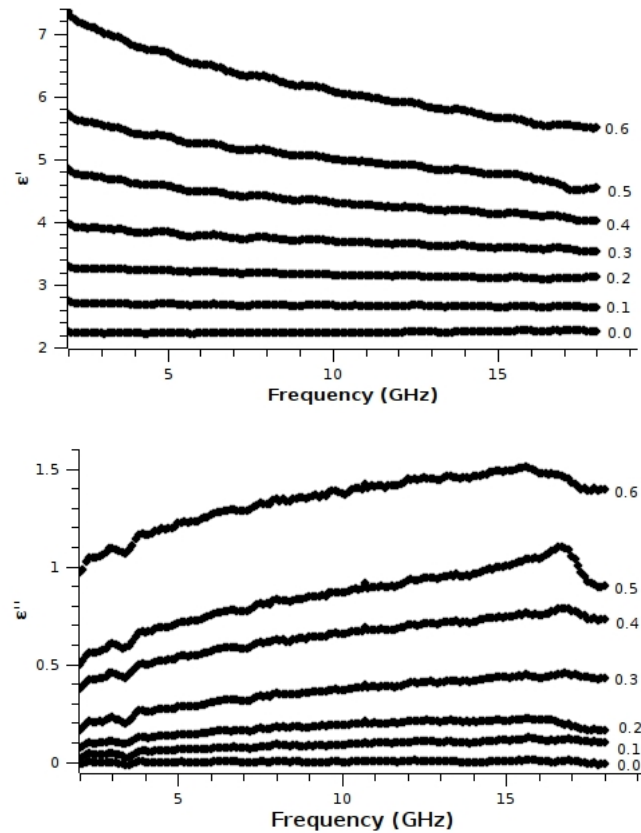**Figure 5.** As for Figure 4 but with AlOx-W-A20-350 filler particles.

Figure 7. As for Figure 4 but with W-A20-350 filler particles.

Table 3. Frequency ν_{max} at which the maximum dielectric loss occurs, peak value ε''_{max}, and the value of ε' at the lowest frequency measured here (2 GHz), corresponding to the measured data shown in Figure 8 for volume fraction $f = 0.6$.

Filler	ν_{max} (GHz)	ε''_{max}	ε'_{2GHz}
AlOx-W-A20-150	14.6 ± 0.5	2.99 ± 0.05	11.7 ± 0.1
AlOx-W-A20-350	16 ± 1	2.2 ± 0.1	10.9 ± 0.1
W-A20-150	14 ± 3	1.3 ± 0.1	6.1 ± 0.4
W-A20-350	15.7 ± 0.3	1.7 ± 0.3	7.8 ± 0.7

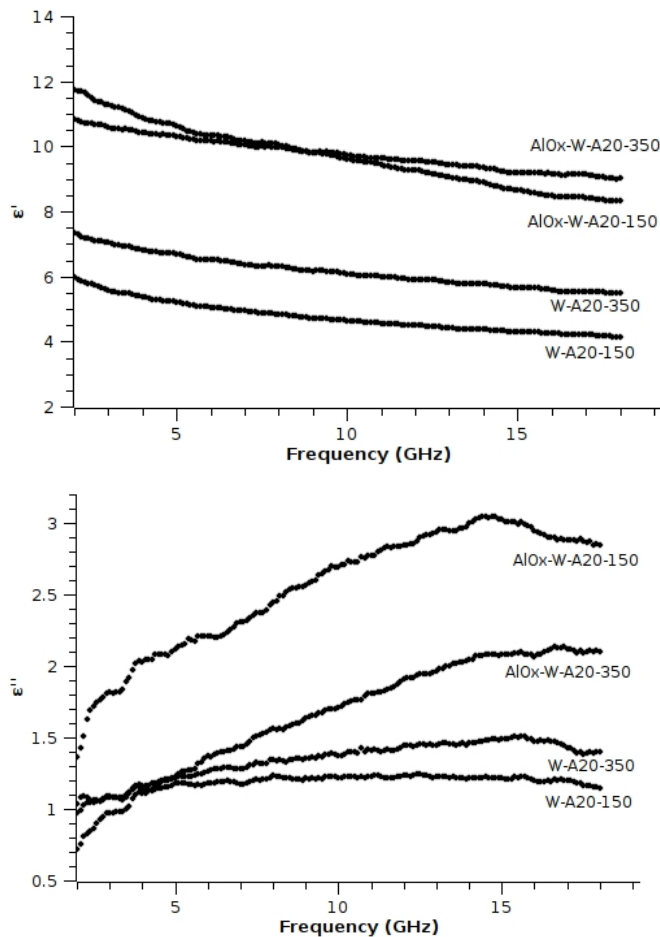**Figure 8.** Measured ε' and ε'' versus frequency for all four filler particle types, with filler volume fraction $f = 0.6$.

itance. There is no significant difference between the frequency of relaxation for filler particles coated with AlOx and those without, Table 3.

3.3 DRYING TEMPERATURE

Figure 8, and parameters extracted from that figure which are given in Table 3, indicate that in the case of composites formed with AlOx-coated particles, ε'' and ε'_{2GHz} are larger for the particles dried at 150 °C than for those dried at 350 °C. These differences are attributed to differences in the morphology of the tungsten coating due to traces of bound water remaining in the Volan® layer of the particles dried at lower temperature [8]. There is no resolvable difference in

the values of ν_{max} for these particles. In the case of non-AlOx-coated particles, neither ν_{max}, ε''_{max} nor ε'_{2GHz} exhibit resolvable difference due to drying temperature.

3.4 MICROSTRUCTURE

In Figure 9, measured permittivity data is shown for three sets of nominally identical samples with W-A20-150 filler particles. These are measurements on samples molded from the same master batch mixture of W-A20-150 filler particles and wax, rather than measurements with newly-prepared particles. At $f = 0.3$ and greater, significant variation in the data is observed for samples with the same volume fraction. The observed variation in measured ε is likely due to microstructural variations from sample to sample, which are known to have a significant effect on bulk material properties such as ε as f increases. Indeed, below $f = 0.3$ the microstructure has little influence on ε for a disperse system. In addition, it is possible that there is some variation in f itself from sample-to-sample, even for samples made from the same master batch mixtures. The ensemble of coated filler particles in any one sample is sufficiently large for effects such as polydispersity of the filler particles, and the distribution of tungsten coating thickness or effective conductivity from particle-to-particle, to give rise to an average response that is similar from sample to sample. For this reason, these effects are likely to play a lesser role in the variations seen in Figure 9 than microstructural variations. The artifact in the data for one sample set, visible at approximately 12 GHz, is the result of instrument calibration error.

3.5 RELAXATION FREQUENCY AND BROADENING

In previous work on smaller glass microbubbles (mean radius 15 μm) sputter-coated with tungsten nominally 20 nm thick and then coated with approximately 3 nm of AlOx, extensive modeling has been undertaken [13, 14]. The findings of those investigations are summarized briefly in this section in order to provide further insight into the dielectric relaxation observed in the measurements presented here.

Modeling the effective permittivity of a composite with multi-layered filler particles by means of an effective medium formulation [4] reveals that the measured relaxation occurs at a frequency several decades lower than that predicted by theory, if the bulk conductivity value of the tungsten is used. If, on the other hand, a reduced value of conductivity is used based on either the assumption of a reduced mean free path for the conduction electrons due to the thin conductive layer [13], or on the observation of the discontinuous nature of the tungsten coating [14], then the modeled relaxation frequency may be reduced to match that measured. For example, in the work of reference [13], a value of tungsten conductivity $\sigma = 2.33$ kS/m was found to yield a match between values of ν_{max} measured and calculated using the effective medium model of reference [4]. The observed relaxation is, however, much broader than that of a simple Debye relaxation predicted by a stand-
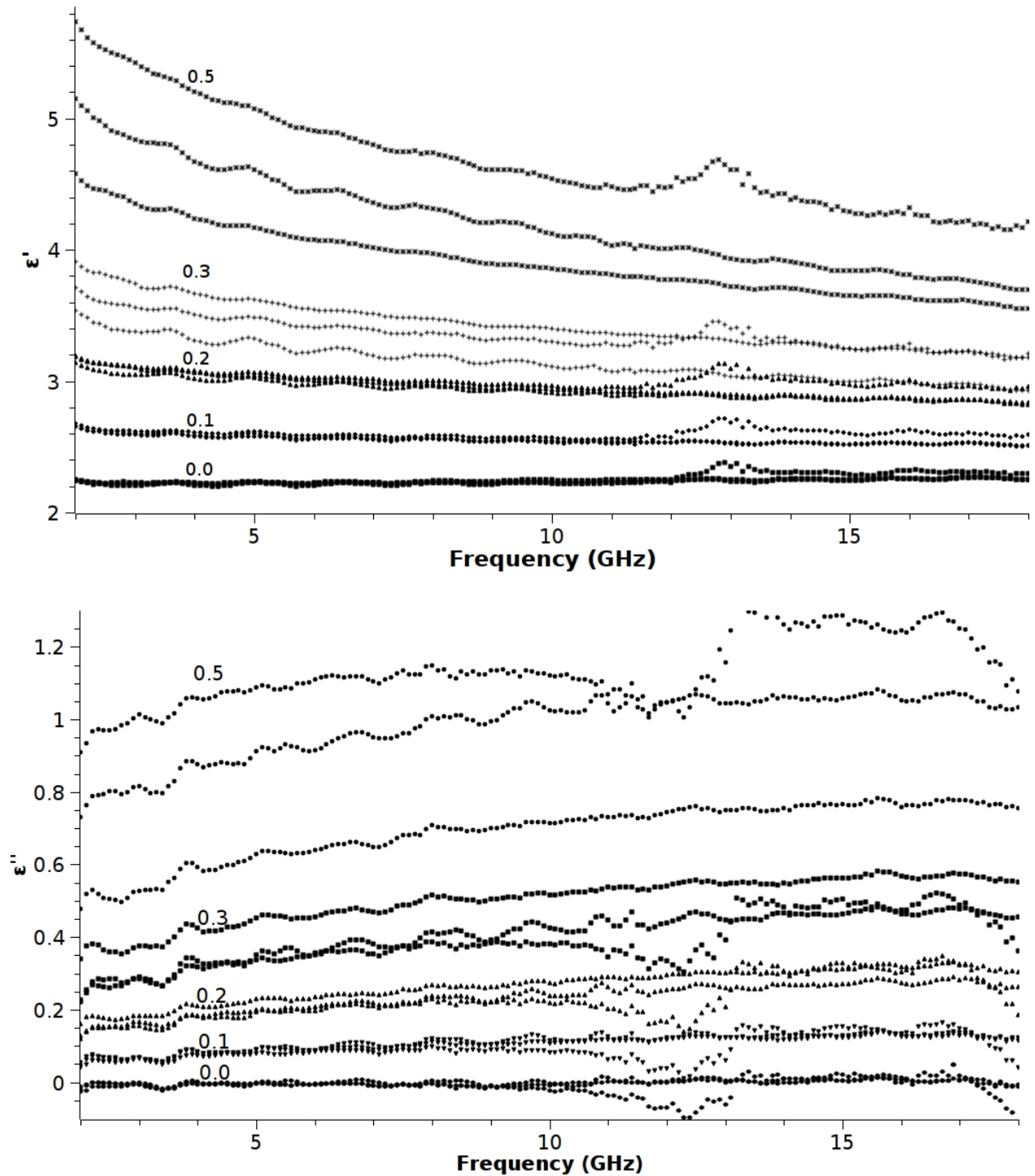
Figure 9. Measured ε' and ε'' versus frequency, comparing three sample sets with W-A20-150 filler particles, for various values of filler volume fraction, f.

ard effective medium treatment, Figure 1. Modeling suggests that the observed broadening of the relaxation is due largely to a distribution of effective metal coating conductivity, due to associated discontinuities in the tungsten layer that vary from particle to particle, rather than the polydispersity of the filler particles [14]. This interpretation is in line with observations on smaller (100–250 nm diameter) metal shells at optical frequencies [15]. Chemical interphase effects due to weak bonding between various species at the particle interfaces may also act to broaden the observed dielectric relaxation, but the species involved (wax and alumina) are basically low-loss dielectrics in this frequency range. This effect is, therefore, expected to be weak in comparison to the effect of variations in the metal coating.

CONCLUSION

Composites made using tungsten-coated glass bubbles (AlOx-W-A20 and W-A20) as filler particles are shown to exhibit dielectric relaxation at frequencies of around 15 GHz and higher, depending on the filler volume fraction. Particles coated with electrically-insulating AlOx exhibit stronger relaxation (larger ε''_{max}) than those without. The effect is more pronounced for higher particle volume fractions due to the closer proximity of the particles permitting charge to leak from one to another when the AlOx insulation layer is not present. For the AlOx-coated particles, the relaxation of samples with particles dried at 150 °C prior to sputter coating with tungsten is somewhat stronger than for those dried at 350 °C. This is attributed to differences in the morphology of the sputtered tungsten coating due to the presence of remaining bound water in the organo-metallic film (Volan®) to which the tungsten adheres.

Composites formed with these layered filler particles are suitable for use as lightweight microwave absorbers due to their dielectric relaxation in the GHz frequency range. Tailoring of the relaxation frequency for a particular application is possible, in principle, by adjustment of the thickness and morphology of the sputtered metal layer [2, 13, 14].

ACKNOWLEDGMENT

REFERENCES

[1] P. S. Neelakanta and J. C. Park, "Microwave absorption by conductor-loaded dielectrics", IEEE Trans. Microwave Theory and Techniques, Vol. 43, 1381-1383, 1995.

[2] N. Bowler, "Designing dielectric loss at microwave frequencies using multi-layered filler particles in a composite", IEEE Trans. Dielectr. Electr. Insul., Vol. 13, pp. 703-711, 2006.

[3] I. V. Antonets, L. N. Kotov, S. V. Nekipelov and Ye. A. Golubev, "Nanostructure and conductivity of thin metal films", Solid State Electronics, Vol. 49, pp. 306-309, 2004.

[4] A. Sihvola and I. V. Lindell, "Polarizability and effective permittivity of layered and continuously inhomogeneous dielectric spheres", J. Electromagnetic Waves and Applications, Vol. 3, pp. 37-60, 1989.

[5] As on 22 July 2006: "3M™ Glass Bubbles A20/1000", http://products3.3m.com/catalog/us/en001/manufacturing_industry/specialty_materials/node_WT7B4GZWNKbe/root_GST1T4S9TCgv/vroot_FG8FTD9L7Wge/gvel_WHB23F5LMRgl/command_AbcPageHandler/theme_us_specialtymaterials_3_0

[6] Potter Industries Inc. Materials Safety Data Sheets for Spheriglass® Glass Spheres A-Glass and E-Glass.

[7] A. Von Hippel, *Dielectric Materials and Applications*, The Technology Press of M.I.T., New York, 1954.

[8] C. S. Chamberlain, Corporate Research Process Laboratory, 3M, St. Paul, MN, personal communication, 2004.

[9] D. Lide, *CRC Handbook of Chemistry and Physics*, CRC Press, Ohio, 2001.

[10] As on 15 July 2006: "Volan®", http://tw.dupont.com/7-a-cse.htm

[11] Volan® Bonding Agent Data Sheet, Dupont.

[12] J. Baker-Jarvis, "Transmission/Reflection and Short-Circuit Line Permittivity Measurements", U.S. Department of Commerce, NIST, 1990.

[13] I. J. Youngs, N. Bowler, K. P. Lymer and S. Hussain, "Dielectric relaxation in metal-coated particles: the dramatic role of nano-scale coatings", J. Phys. D: Appl. Phys., Vol. 38, 188-201, 2005.

[14] I. J. Youngs, N. Bowler and O. Ugurlu, "Dielectric relaxation in composites containing electrically isolated particles with thin semi-continuous metal coatings", J. Phys. D: Appl. Phys., Vol. 39, 1312-1325, 2006.

[15] S. L. Westcott, J. B. Jackson, C. Radloff and N. J. Halas, "Relative contributions to the plasmon line shape of metal nanoshells", Phys. Rev. B, Vol. 66, 155431, 2002.

Thomas C. Maloney was born in Cincinnati, Ohio, U.S.A. in 1984. He graduated with the B.Sc. degree in 2007 from the University of Cincinnati and is now working on his Ph.D. degree in physics there. In 2006 he completed a summer internship at the Laboratori Nazionali di Frascati in Frascati, Italy where he investigated Reliable Resistive Plate Chambers (R^{2}PC).

Nicola Bowler (M'99-SM'02) was born on 6 December 1968 in Hereford, England. She received a B.Sc. degree in physics from the University of Nottingham, UK, in 1990 and the Ph.D. degree from the University of Surrey, UK, in 1994, for theoretical work in the field of eddy-current nondestructive evaluation (NDE). Since 1997 she has broadened her interests in applied electromagnetism to include dielectric and magnetic behavior of composite materials. She moved to the Center for NDE, Iowa State University, in 1999 and in 2006 was appointed Associate Professor of Materials Science and Engineering at Iowa State University.

Nathan L. Fischer was born on 19 March 1985 and raised on a farm near Neola, Iowa, U.S.A. He is currently working toward a concurrent BS/MS degree in Materials Science and Engineering from Iowa State University. Current research includes the microwave properties of dielectric composites, electroless metal deposition, and powder characterization techniques. Other academic interests include German, theology, and music.